Sloshing Suppression Control of Liquid Transfer Systems Considering a 3-D Transfer Path

Ken'ichi Yano, *Member, IEEE,* and Kazuhiko Terashima, *Member, IEEE*

***Abstract*—In plants in many industries, there exist a lot of transfer systems with vibration mechanisms. While transfer without residual vibration is usually demanded in these plants, this requirement necessitates large numbers of sensors and complicated models for control design. Therefore, this paper presents a trajectory control design method to suppress residual vibration in transfer systems without the need to directly measure vibration. The proposed method consists of two parts. First, the frequency characteristics of the controller, comprised of control elements with simple structures such as a notch filter and a low-pass filter, are shaped as needed to suppress vibration. Next, various parameters of the control elements are determined by solving an optimization problem with penalty terms expressed by the constraints of both the time and frequency domains. The proposed method is applied to a liquid container transfer system, with special consideration given to the suppression of sloshing (liquid vibration) as well as to the maintenance of a high-speed transfer on the container's three-dimensional transfer path. The obtained controller demonstrates good performance for all demands. The effectiveness of the control design method is shown by experiments.**

***Index Terms*—Casting process, manufacturing automation, optimization methods, sloshing, vibration control.**

I. Introduction

SLOSH suppression problems have recently become of great importance in various fields. Significant areas of investigation include liquid container transfer systems such as those used to transfer molten metal from a furnace [1]–[3], motion control for automatic pouring [4]–[6] in the casting and steel industries, the operation of a machine that packages fluids [7], [8], as well as the transfer of perfume in perfume manufacture and beer in the beverage industry. Furthermore, liquid container transfer systems have been developed to replace pipelines in the chemical and food industries. In practical industries such as these, it is essential to avoid overflow caused by sloshing, as well as to prevent any deterioration in quality due to contamination. It is also important to shorten the total operational time in order to improve productivity.

In present conditions in real plants, transfer systems have moved slowly to prevent vibration or else have required expert operators. In fact, these practices have prevented improvements in productivity and safety. Therefore, it is necessary to construct a liquid container transfer system that will suppress sloshing as well as facilitate high-speed transfer.

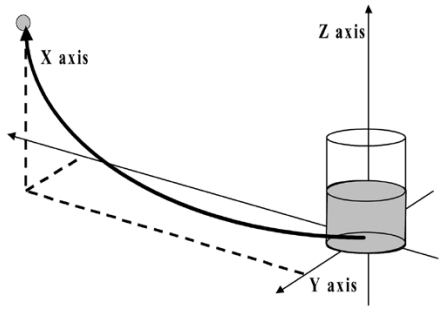

Fig. 1. Illustration of the liquid container transfer control on a 3-D transfer path.

With respect to the shapes and transfer paths of the containers, historically either narrow or three-dimensional (3-D) rectangular containers on a straight path have been studied. By contrast, in recent years, the transfer of cylindrical containers and transfers involving curved paths have been of increasing interest [9]. Studies in more recent years have focused on advanced control of liquid container transfer, paying special attention to inclined transfer paths and to slosh suppression [10].

However, there are no studies on a liquid container transfer system that can freely transfer a container in 3-D space as shown in Fig. 1, although such a system would be very important and effective in realizing space-saving factories, optimizing production processes, and improving productivity in real industries. From those perspectives, the demand for such a system would be obvious.

In contrast, the analysis and modeling of 3-D fluid dynamics are very complicated. The Computational Fluid Dynamics (CFD) model, which is a distributed parameter system, is well known as a good tool for analyzing 3-D fluid dynamics. However, it is unsuitable as a control system design model and is difficult to use for real-time control, although it is useful for simulating the fluid behavior. In addition, the CFD model is expressed by complicated equations, and, when it is directly exchanged to a lumped parameter system for the control system design, it will have a huge number of orders. Furthermore, in some cases, the sensors that are needed to capture the necessary vibration data itself may be uninstallable for the real-time control. Even if the sensors can be installed, the installation would increase costs. It is also difficult to identify the model parameters in a real process, such as the equivalent coefficients of viscosity, of the lumped parameter model [1], because the molten metal is at a high temperature.

Manuscript received August 3, 2002; revised December 29, 2003, and May 11, 2004.

K. Yano is with the Department of Mechanical and Systems Engineering, Gifu University, Gifu 501-1193, Japan (e-mail: yano@procon.tutpse.tut.ac.jp).

K. Terashima is with the Department of Production Systems Engineering, Toyohashi University of Technology, Aichi 441-8580, Japan (e-mail: terasima@procon.tutpse.tut.ac.jp).

Digital Object Identifier 10.1109/TMECH.2004.839033

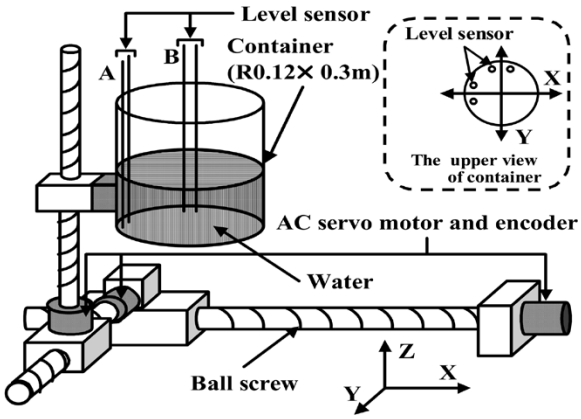

Fig. 2. Schematic diagram of the experimental apparatus for the liquid container transfer control on a 3-D transfer path.

Therefore, the purpose of this paper is to develop a liquid container transfer system with a 3-D transfer path that suppresses sloshing without vibration feedback. Furthermore, a controller is found that allows the container to be transferred as fast as possible while meeting the given control specifications. In the design, a design method for trajectory control with vibration damping that satisfies various hybrid specifications in the frequency domain (e.g., gain margin, phase margin, and vibration characteristics) and the time domain (e.g., transient response, settling time, overshoot, and constraint of control input) by using feedback of only the container's position, is applied. The setup has three independent motion capabilities, which restricted the research even more to three times SiSo-control in stead of MiMo-control, although it is shown that the sloshing in different direction is independent at the end of this paper.

This paper is organized as follows. Section II presents the details of the liquid container transfer system. In Section III, the problem statement, design problem, and the design procedure are described, and the proposed control system is constructed. Then the effectiveness of the proposed 3-D liquid container transfer system is shown by experiments in Section IV. Furthermore, at the end of this paper, the interference of sloshing in the 3-D transfer is discussed in Section IV.

II. Experimental Apparatus

A schematic diagram and a photograph of an experimental apparatus are shown in Figs. 2 and 3, respectively. In this study, the 3-D cylindrical container, which is generally used in real industries in the casting process, is used, because the cylindrical container keeps the molten metal hot for a long time compared with a fan-type container. The radius of the container R is 0.12 m and its height is 0.3 m. The static liquid level h_s is 0.16 m. A 3-D transfer path is used.

The object liquid in the experiment is water. Even if the real plants in casting industries are considered, it is possible to use water in this study, because the Reynolds' number of water at normal temperatures is almost the same as that of molten iron or molten aluminum at high temperatures considering the similarity law in fluid dynamics. For example, the kinematic viscosities of molten iron metal at 1350 and 1400 K are 1.365×10^{-6} [mPa $\cdot$ s] and 1.237×10^{-6}[mPa $\cdot$ s], respectively, while that of water is 1.0×10^{-6} [mPa $\cdot$ s] at 293 K [4]. Then the fluid behavior of molten metal may be fairly predicted by water analysis.

The container is moved using ac servo motors with ball screws. The velocity and position of the container are controlled by means of voltage applied to the motors on the X, Y, and Z axes, one motor per axis. The position of the container in 3-D space is detected by three encoders fitted to each axis. In order only to evaluate the experimental results, two-level sensors were installed on this apparatus, as shown in Fig. 2. One is set near the side wall of the X axis (Sensor A), and the other is set near the side wall of the Y axis (Sensor B), because the first-order mode sloshing caused by the movement of the X and Y axes can be observed most distinctly near the side wall of the container. Displacement of the liquid level is detected through changes in resistance between two stainless electrodes. The specifications of ac servo motors and encoders are shown in Table I, where R_o is the rated output (kW), M_v is the maximum turning velocity (rpm), and O_p is the output pulse (P/R).

For the ac servo motor on each axis, the transfer function $G_m(s)$ from the input voltage $e(t)$ to the position $y(t)$ of the container is given as the following first-order lag model with an integrator:

$$G_m(s) = \frac{Y(s)}{E(s)} = \frac{K_m}{s(T_m s + 1)} \tag{1}$$

where T_m (s) is the time constant and K_m (m/sV) is the gain. These parameters were obtained by adding a stepwise input to the apparatus. As a result, the parameters on each axis were obtained as shown in Table II, where the maximum velocity $V_{\max}$ (m/s) and maximum acceleration $A_{\max}$ (m/s^2) of each motor are also shown in the table.

In general, the natural frequency f_n of the perfect fluid in a cylindrical container is analytically represented by the following equation [9]:

$$f_n = \frac{1}{2\pi}\sqrt{\frac{g}{R}\epsilon_1 \tanh\left(\epsilon_1 \frac{h_s}{R}\right)} \tag{2}$$

where h_s is the static liquid level, R is the radius of a cylindrical container, g is the gravitational acceleration, and ϵ_1 is the least positive root for the first-order derivative of the first Bessel function ($\epsilon_1 = 1.841$). The target liquid level h_s is 0.16 m and the radius of the cylindrical container is $R = 0.12$ m in this study. Hence, the natural frequency f_n is calculated as 1.9379 Hz (12.17 rad/s). This natural frequency will be held even if the container is transferred to any direction in 3-D space.

III. Control System Design

A. Problem Statement and Design Problem

Modern control theory by optimal regulators [3] and robust control theory by H_∞ control [1] have both been applied to liquid container transfer systems. The former could neither realize loop-shaping in the frequency domain nor guarantee the robustness for the model uncertainty. The latter, meanwhile,

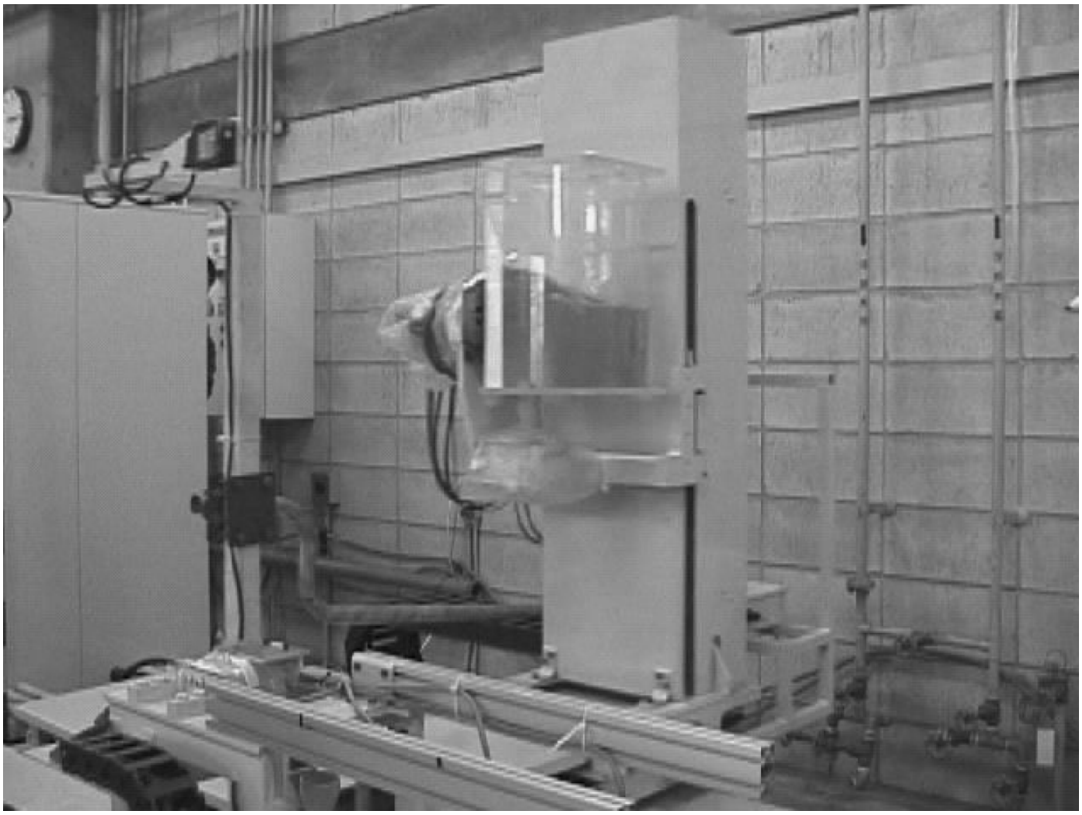

Fig. 3. Photograph of the experimental apparatus for the liquid container transfer control on a 3-D transfer path.

TABLE I
SPECIFICATIONS OF AC SERVO MOTORS

	R_o	M_v	O_p
X-axis	2.90	1500	16384(16bit)
Y-axis	0.40	3000	16384(16bit)
Z-axis	0.75	3000	16384(16bit)

TABLE II
MOTOR PARAMETERS

	K_m	T_m	V_{max}	A_{max}
X-axis	0.1670	0.0130	0.8	2.0
Y-axis	0.0838	0.0089	0.5	1.0
Z-axis	0.0850	0.0182	0.5	1.0

could not clearly shape the transient response, required a long time to tune the weighting matrices, and made the dimensions of the controller high. In fact, the sloshing (liquid vibration) of a liquid container transfer system is caused by self-transfer movement under circumstances without a disturbance. Therefore, it is theoretically possible to suppress the vibration by controlling the acceleration of the transfer, thereby obviating the need to directly measure vibration [11], [12].

In the control design for the system that causes vibration by the self-transfer movement, it is important to shape the controller's frequency characteristics into the notch-typed one at the resonance frequency, in order to suppress sloshing. It is also important to shape the controller's frequency characteristics at the other frequency region in order to satisfy the specifications in the time domain, such as transient response. Therefore, for the trajectory control of a transfer system with vibration damping, it

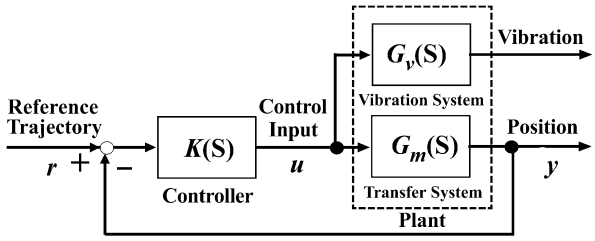

Fig. 4. Target closed-loop system for the proposed approach.

is very useful to directly shape the loop transfer function or the closed-loop transfer function by using a controller comprised of control elements with simple structures, such as a notch filter and a low-pass filter, whereas H_∞ control indirectly shapes the frequency characteristics by using high-order weighting functions.

In this approach, a controller is given as a set of simple elements so that the control object is to design a position control system with vibration damping. The controller is automatically calculated by solving the optimization problem with penalty terms that are quantitatively expressed by the specifications in both the time and frequency domains. The closed-loop system with the block diagram shown in Fig. 4 is considered. This is a servo system that makes the position y of the output follow the reference trajectory r. The controlled system $G_m(s)$ denotes the transfer system, $G_v(s)$ denotes the vibration system, and $K(s)$ denotes the controller.

This control design problem is "to design a transfer system that suppresses vibration as well as facilitates high-speed

transfer." The designed control system does not conduct feedback of the vibration data. There are many application fields for such a system in real plants. For example, in a crane system, the transfer system is a cart that moves a load and the vibration system is a rope with a load. In a robotic arm, the transfer system is a motor that moves each joint and the vibration system is a tip of an arm. In this paper, the present approach is called the hybrid shape approach, because the controller is designed to reasonably satisfy the hybrid specifications for time and frequency characteristics simultaneously.

B. Design Procedure

The procedure to design the controller of the hybrid shape system is comprised of the following four steps.

Step 1) *Selection of the controller elements*:
Select prerequisite controller elements for the control specifications, such as proportional gain, integral gain, derivative gain, low-pass filter, and notch filter. Construct a controller in terms of the several fundamental control elements.

Step 2) *Formulation of design specifications*:
Represent the design specifications in the frequency domain (e.g., gain margin, phase margin, and vibration characteristics) and the time domain (e.g., transient response, settling time, maximum overshoot, and constraint of control input) by using penalty functions.

Step 3) *Formulation of an optimization problem*:
Formulate the optimization problem with constraints expressed as penalty terms.

Step 4) *Computation of the controller*:
Adjust the parameters of the controller by solving the optimization problem.

The container is independently transferred in the X, Y, and Z directions on the present apparatus. Therefore, the controllers can be independently designed on each axis. The controllers on the X and Y axes are designed considering both the characteristics of the motors and the resonance frequency of the sloshing. On the other hand, since the movement in the Z direction does not influence sloshing, the controller on the Z axis can be designed considering only the characteristics of the motor. Details of each item of the design procedure are shown below. Interference on each axis will be discussed in Section V.

C. Selection of Controller's Elements

In order to satisfy the desirable control specifications, the controller is formulated as

$$K(s) = \prod_{i=1}^{n} K_i(s). \tag{3}$$

This makes it possible to design a controller satisfying various control specifications by selecting multiple controller elements $K_i(s)$, unless the number of parameters is high.

Equation (1) is a servo system with an integrator. Thus, according to the internal model principle, it is sufficient to use a proportional control (P control) system to avoid the offset. Therefore, a proportional gain (K_1) is selected as the first element of the controller $K(s)$ given by (3) on each axis to yield

$$K_1(s) = K_P. \tag{4}$$

In order to reduce the influence of the higher mode sloshing and noise, a low-pass filter (K_2), which makes the controller low gain at high-frequency domain, is selected as the second element of the controller on each axis

$$K_2 = \frac{1}{T_l s + 1}. \tag{5}$$

For the controllers on the X and Y axes, a notch filter (K_3) is selected as the final element of the controller in order to suppress the sloshing

$$K_3 = \frac{s^2 + 2\zeta\omega_n s + \omega_n^2}{s^2 + \omega_n s + \omega_n^2}. \tag{6}$$

It is known that the dominant mode of the sloshing in the container is a first mode [1], [3]. When the static liquid level h_s is 0.16 m, the first-mode natural frequency is $f_n = 12.17$ rad/s (1.9379 Hz). Therefore, the parameters ω_n and ζ in (6) are given as $\omega_n = 12.17$ and $\zeta = 0.0001$, respectively. By introducing the notch filter into the controller $K(s)$, the controller gain can be relatively shaped to be at least 20 dB lower at the natural frequency of the sloshing. The notch filter also allows for the suppression of residual vibration without direct measurement of the liquid vibration.

Finally, the transfer functions of the controllers on the X and Y axes are given as

$$\begin{aligned} K_x(s), K_y(s) &= \prod_{i=1}^{3} K_i \\ &= \frac{K_P(s^2 + 2\zeta\omega_n s + {\omega_n}^2)}{(T_l s + 1)(s^2 + \omega_n s + {\omega_n}^2)} \end{aligned} \tag{7}$$

and that of the controller on the Z axis is given as

$$K_z(s) = \prod_{i=1}^{2} K_i = \frac{K_P}{T_l s + 1}. \tag{8}$$

In (7) and (8), K_P and T_l are unknown parameters. These parameters are reasonably determined by solving an optimization problem.

D. Formulation of Design Specifications

In this approach, various control specifications in both the time and frequency domains can be given. The specifications of the controllers in both domains are formulated using penalty functions, and then the controllers $K_x(s)$, $K_y(s)$, and $K_z(s)$ are, respectively, calculated to satisfy the specifications. In this control design, Specs. (I)–(V) shown below were given, where Specs. (I)–(IV) apply to every controller while Spec. (V) is for the controllers on the X and Y axes only.

- Spec. (I) : The controller and closed-loop system are stable. Penalties are given in order to compensate for the stabilities of the controller and closed-loop system, if the following relations are unsatisfied:

$$\begin{aligned} \mathrm{Re}[r_K] &< 0 \\ \mathrm{Re}[r_{\mathrm{cl}}] &< 0 \end{aligned} \tag{9}$$

$$\begin{aligned} K_P &> 0 \\ T_l &> 0 \end{aligned} \tag{10}$$

where r_K and r_{cl} are the characteristic roots of the controller and those of the closed loop, respectively.

- Spec. (II) : The controller gain is less than 0 dB at $f_h = 314$ rad/s (50 Hz), in order to decrease the influence of the higher order sloshing mode and noise. Penalties are given if the following relation is unsatisfied:

$$|K(f_h)| < 0 \text{ (dB)}. \tag{11}$$

- Spec. (III) : The input voltage u does not exceed the magnitude of ± 10 V due to the hardware constraint. Penalties are given if the following relation is unsatisfied:

$$\max|u| < 10 \text{ V}. \tag{12}$$

- Spec. (IV) : Maximum overshoot does not exceed the magnitude of 10^{-3} m. Penalties are given if the following relation is unsatisfied:

$$\max(O_s) < 10^{-3} \text{ m}. \tag{13}$$

- Spec. (V) : The controller gain is less than 0 dB at the first-mode natural frequency $f_n = 12.17$ rad/s. Penalties are given if the following relation is unsatisfied:

$$|K(f_n)| < 0 \text{ dB}. \tag{14}$$

Of course, other control specifications can be added in this approach: for example, frequency specifications on a closed-loop system and specifications in the time domain such as rise time, delay time, recovery time, and settling time.

E. Formulation of an Optimization Problem

Parameters of controllers are obtained by minimizing the cost function expressed as

$$J = T_s + J_p. \tag{15}$$

In (15), T_s is the settling time of the transfer expressed as follows:

$$T_s = \min\{t|\ |y_f - y(t+\sigma)| < y_e,\ \sigma \geq 0\} \tag{16}$$

where y is the position of the container at time t and y_f is the target point. Therefore, T_s is the settling time for the reference trajectory r. y_e is the admissible error for the target position which is set to 10^{-3}, and J_p is the penalty term expressed as

$$J_p = w_1 + w_2 + \cdots + w_i + \cdots \tag{17}$$

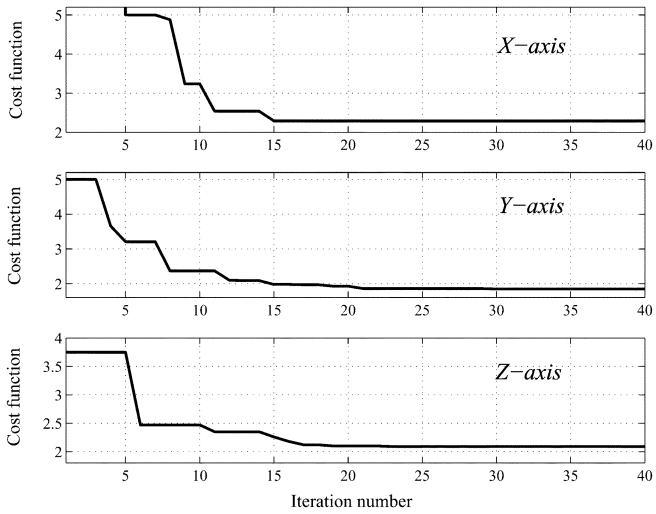

Fig. 5. Results of the optimization of the cost function on each axis.

where w_i is the penalty. Each time the penalty conditions hold, the penalty $w_i = 10^8$, which is big enough to avoid the penalty conditions, will be added to satisfy the control specifications.

In order to obtain the controller $K(s)$, the optimization problem with the constraints is formulated with: target function (the settling time of the transfer $T_s \longrightarrow$ minimum) and constraints (9)–(14).

F. Computation of a Controller

Finally, the unknown parameters in the controller $K(s)$ given in (3) are computed by solving the optimization problem with the constraints expressed in (15).

To optimize the cost function, the simplex method [13] is applied to the present problem, because the number of unknown parameters are only two in this case, where the reflection coefficient $\alpha = 1.0$, the expansion coefficient $\beta = 0.5$, and the contraction coefficient $\gamma = 2.0$. The solution by the simplex method is not always the global optimal solution. Hence, the initial simplex values and the weights of the cost function are modified to obtain the desirable characteristics of the controller. The initial simplex values were $K_P = (25, 160, 20)$ and $T_l = (0.01, 0.005, 0.1)$ for the X axis, $K_P = (40, 110, 20)$ and $T_l = (0.01, 0.005, 0.1)$ for the Y axis, and $K_P = (25, 70, 20)$ and $T_l = (0.01, 0.005, 0.1)$ for the Z axis. The reference trajectory in Fig. 4 was separately determined by integrating the maximum velocity and maximum acceleration of the present experimental apparatus on each axis. In the design, the starting point was set to $(x, y, z) = (0, 0, 0)$ m and the endpoint was $(x, y, z) = (1.0, 0.3, 0.5)$ m because of the limitations of the apparatus.

In Fig. 5, the results of the optimization of the cost function on each axis are shown. As a result of the computations, the number of iterations of the convergence is around 20, and it took approximately 20 s to compute all of the optimization problems by using a personal computer (Pentium III 600-MHz CPU), as shown in Fig. 5. The characteristic roots of the closed-loop controller are stable, because all of their real parts have become negative. Table III shows the results of the computations.

TABLE III
VALUES OF COST FUNCTIONS AND PARAMETERS OF THE OBTAINED CONTROLLER ON EACH AXIS

	$J = T_s$	K_p	T_l
X axis	2.29	15.29	0.052
Y axis	1.85	26.05	0.083
Z axis	2.09	33.21	0.107

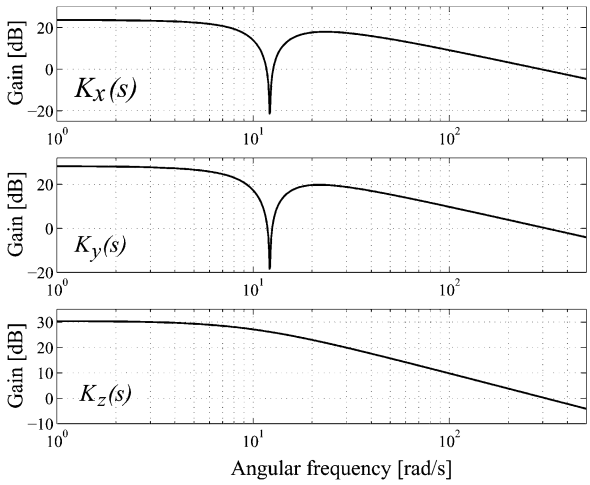

Fig. 6. Bode diagram of the proposed controllers.

The frequency responses of the controllers are shown in Fig. 6. From the figures of $K_x(s)$ and $K_y(s)$, it can be seen that the gains decrease at the resonance frequency (12.17 rad/s) of the sloshing; the specification is satisfied because they are less than 0 dB. Also, it can be confirmed that they are less than 0 dB at $f_h = 314$ rad/s (50 Hz) from the figures of all the controllers. Since the gains are monotonously decreasing in the high frequency domain, it is also clear that these controllers can reduce the influence of high-mode sloshing and noise. The high-speed transfer of the container is also achieved because the gain of the controller is high in the low frequency domain.

Furthermore, the validity of the optimization on each axis is clear because the gains at $f_h = 314$ rad/s are designed as nearly highest gain in the limitation 0 dB such as -0.64 dB on the X axis, -0.02 dB on the Y axis, and -0.08 dB on the Z axis.

From the simulation results of the container transfer obtained by using these controllers, it was confirmed that overshoot was not found and the constraint of control input was satisfied. On the other hand, regarding the sloshing simulation, the CFD model was used in order only to evaluate the control results for the sloshing. The results of both the container transfer and fluid behavior can be evaluated by the experimental results shown in Section IV, because the experimental results are almost the same as the simulation results.

IV. EXPERIMENTAL RESULTS

In Figs. 7 and 8, the experimental results of the proportional control (P control) without a notch filter are shown for the sake of comparison with the results of the proposed Hybrid shape approach. The proportional gains of the X, Y, and Z axes were set to $K_P = 34.0$, 55.5, and 61.5, respectively, in order to have

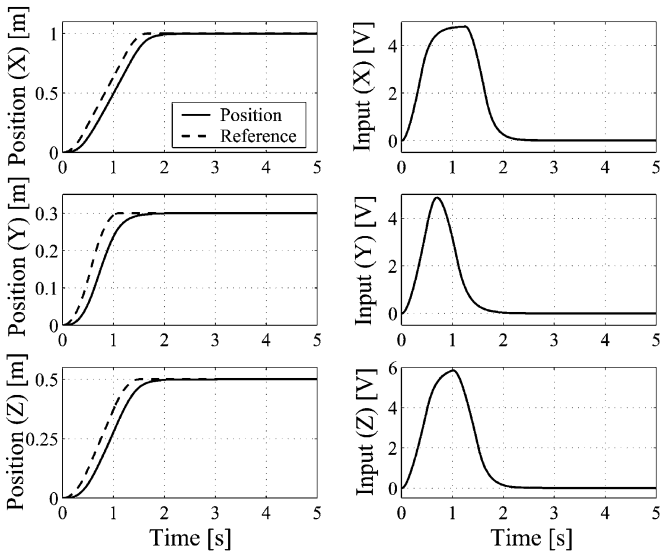

Fig. 7. Experimental result of container transfer on a 3-D transfer path by the P control.

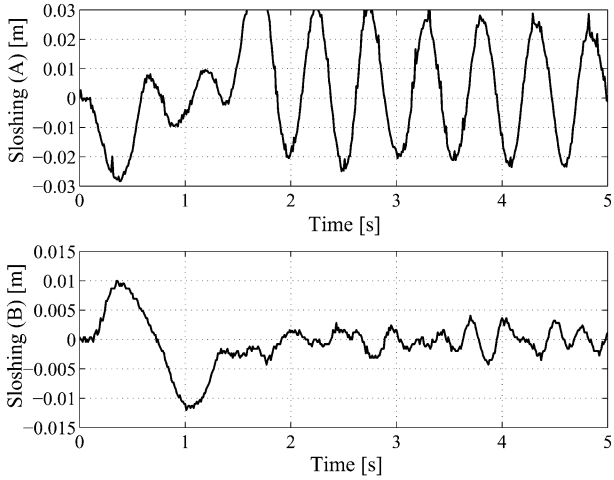

Fig. 8. Sloshing result by the transfer of Fig. 7.

the same settling time that was obtained with the result of the Hybrid shape approach. The positions and control inputs of the X, Y, and Z axes are shown in Fig. 7, and the sloshing detected by the two-level sensors which are expressed in Fig. 2 is shown in Fig. 8, where Sloshing (A) and Sloshing (B) are the sensor outputs from the level sensors A and B shown in Fig. 2, respectively. Namely, Sloshing (A) and Sloshing (B) show the sloshing behaviors in the directions of the X and Y axes, respectively.

As seen from Figs. 7 and 8, positioning control is achieved, but the container transfer causes a lot of sloshing, where the reason that the sloshing on X axis is much bigger than that on Y axis is related to their transfer time and transfer distance. On the other hand, it is realized that the position control is achieved in 3-D space without overshoot, and sloshing is suppressed in both directions by the Hybrid shape approach, as shown in Figs. 9–11. Furthermore, observation of the transfer confirmed that there was no swirling phenomenon in the sloshing, and no interference of any of the movements on any of the axes

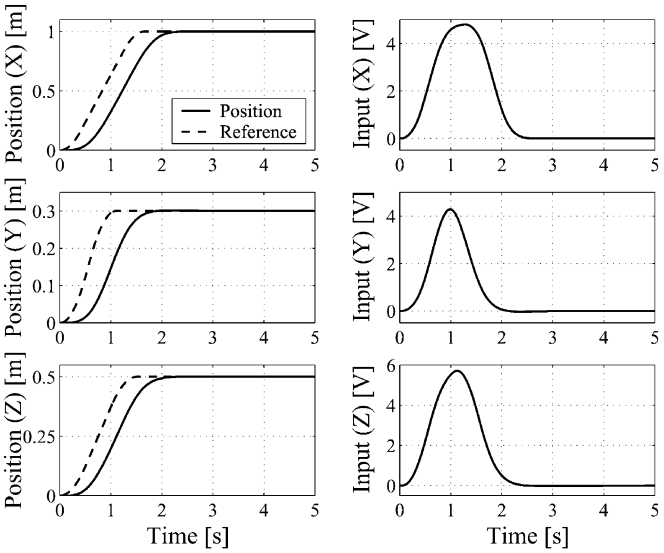

Fig. 9. Experimental result of container transfer on a 3-D transfer path by the Hybrid shape approach.

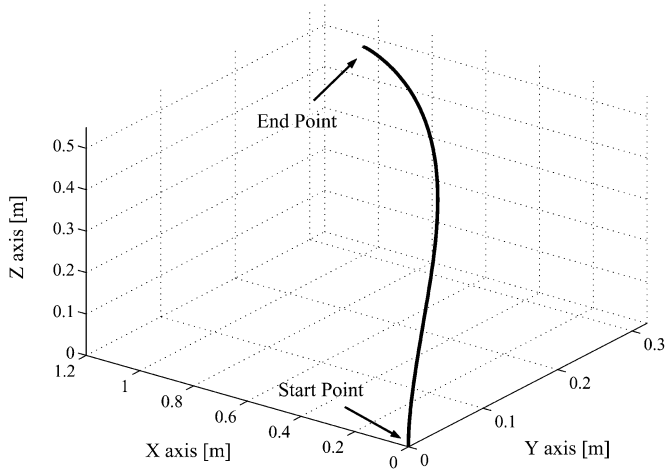

Fig. 10. Trajectory of 3-D transfer by the Hybrid shape approach.

although the container was transferred on the 3-D curved path, as shown in Fig. 10.

By comparison with the result of the H_∞ control in the previous study [1], an almost equivalent control performance was obtained using the Hybrid shape approach. In addition, the overshoot-free characteristic is easily obtained by the proposed approach, whereas this characteristic was very difficult to get by the H_∞ control. Further, the order of the controller in the proposed method could be lower than that of the H_∞ controller.

V. Discussion on the Interference of Sloshing in the 3-D Transfer

In this section, we discuss the interference that occurs in the fluid behavior by the 3-D movement. First, the influence of sloshing that occurs by the container transfer toward the X axis on sloshing toward the Y axis was investigated and vice versa. As the trajectory, the starting point was set to $(x, y, z) = (0, 0, 0)$ m, and the endpoint was $(x, y, z) = (0.3, 0.3, 0)$ m. The experimental result obtained

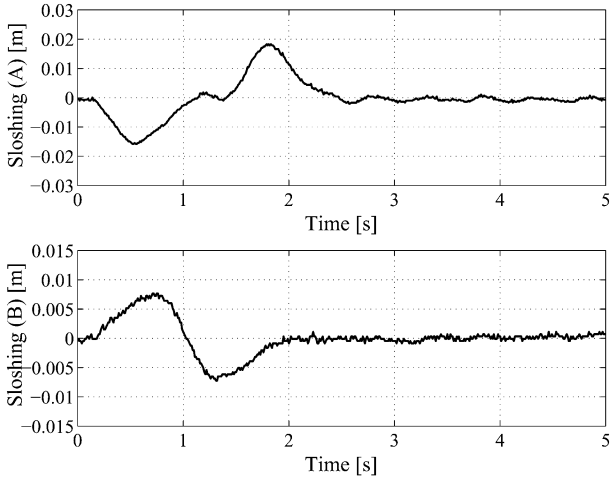

Fig. 11. Sloshing result by the transfer of Fig. 9.

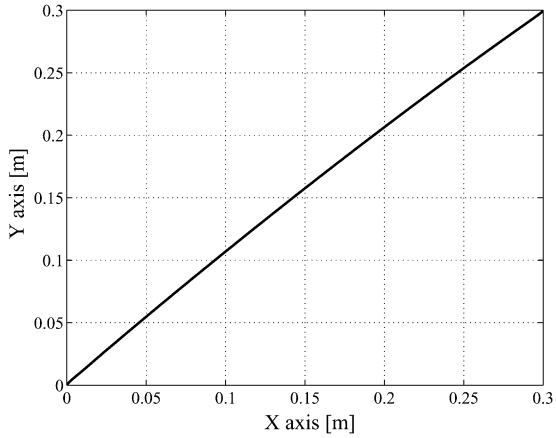

Fig. 12. Trajectory of 2-D transfer for X and Y directions by the P control.

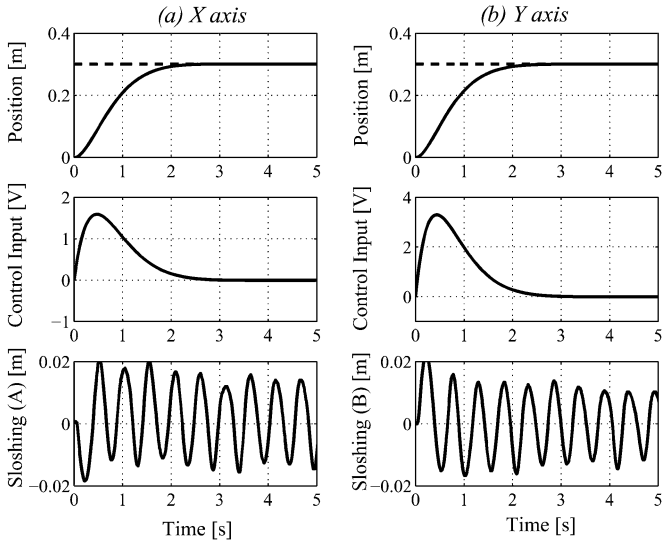

Fig. 13. Experimental results of the position, input, and sloshing on each axis.

without a notch filter in (7) is shown in Figs. 12 and 13. In this case, the reference trajectories on each axis were given as a step input, in order to amplify the sloshing phenomenon. The trajectory on the X–Y plane is shown in Fig. 12, and the position, input, and sloshing on each axis are shown in Fig. 13.

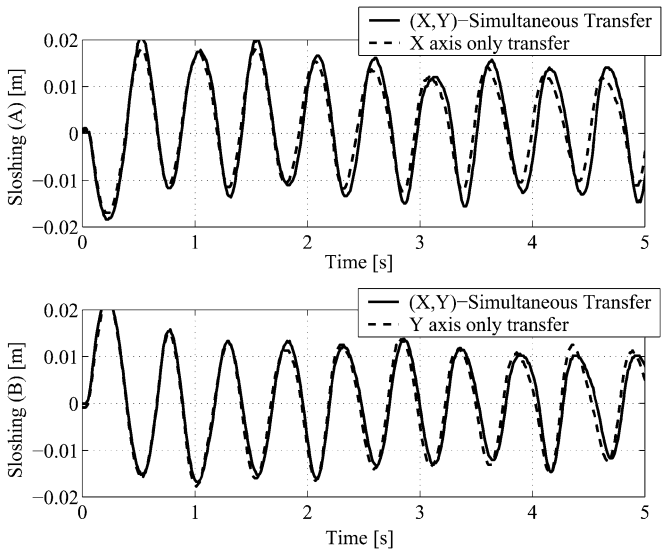

Fig. 14. Sloshing results of the (X, Y)-simultaneous transfer on X–Y plane and straight transfer on only the X axis and on only the Y axis.

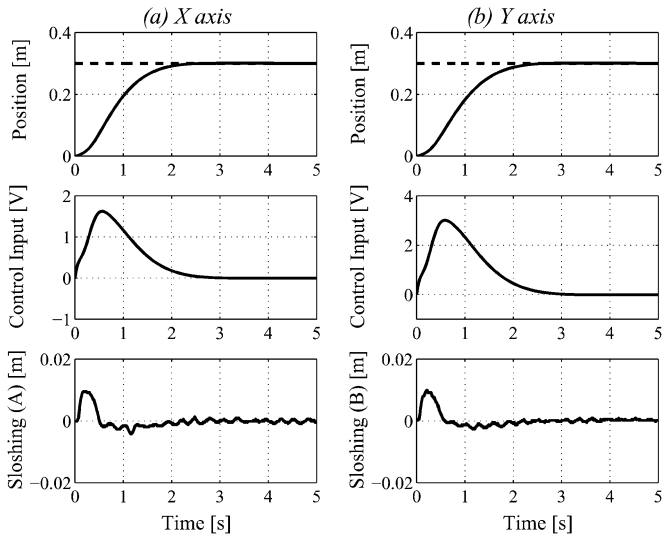

Fig. 15. Experimental result of the (X, Y)-simultaneous transfer by Hybrid shape approach.

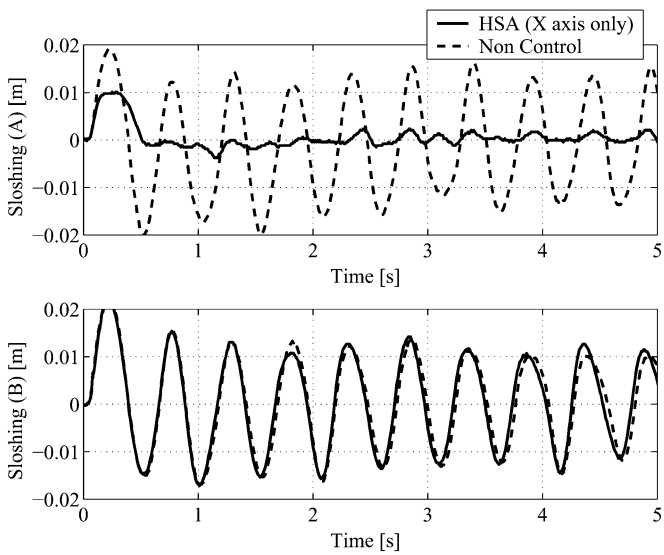

Fig. 16. Reconfirmation experiments of whether or not the controllers can be independently designed on each axis.

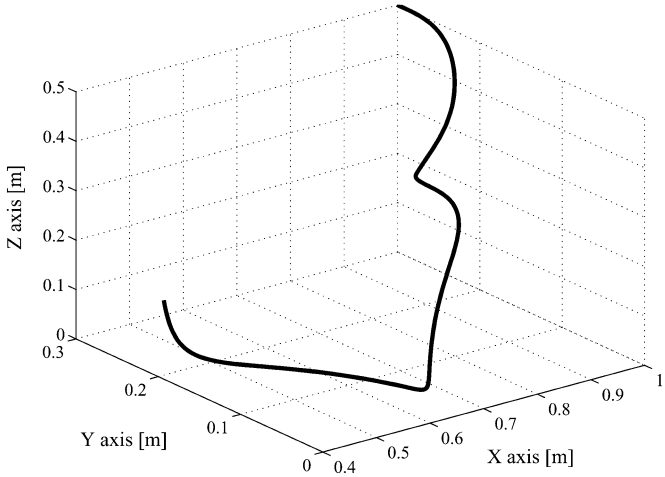

Fig. 17. Trajectory of 3-D transfer by the Hybrid shape approach for random reference endpoints.

As seen from these figures, positioning control was achieved, but the container transfer caused a lot of sloshing on both axes.

Next, in order to check the interference that occurs in the transfer, experiments in which the container was transferred on only the X axis or on only the Y axis were respectively conducted. In Fig. 14, the sloshing results that were plotted with the results of Fig. 13 are shown.

From these experiments, the sloshing behaviors obtained by sensors A and B were almost the same in the (X, Y)-simultaneous transfer and the one-axis transfer, although the container was straightly transferred on only the X axis or on only the Y axis. Therefore, it was found that, with a cylindrical container, there is little interference in the transfer on the X–Y plane. Of course, in all cases, it is also possible to suppress the sloshing by the proposed method, as shown in Fig. 15.

Furthermore, in order to reconfirm that the controllers can be independently designed on each axis, the controller on the X axis was only designed by the Hybrid shape approach. The result is shown in Fig. 16.

As a result, it can be seen that the sloshing on the X axis only is suppressed, even though the sloshing still occurred on the Y axis with the same amplitude and frequency. From these results, it can be said that the controllers can be independently designed on each axis. In other words, this proposed method can suppress the sloshing on the desired axis.

Finally, Figs. 17–19 show experimental results of the container transfer by the Hybrid shape approach and by the P control for the cases of random reference endpoints, respectively. The random reference endpoints were given after the transfer shown in Figs. 7–11 in order to know the influence of the continuous 3-D movement of the container as used in real plants.

As shown in Figs. 17 and 18, even though the container was freely transferred in 3-D space, the sloshing was suppressed at each point along each axis by using the proposed Hybrid shape approach. On the other hand, the sloshing was quite excited by the continuous transfer in the case of the P control (Fig. 19).

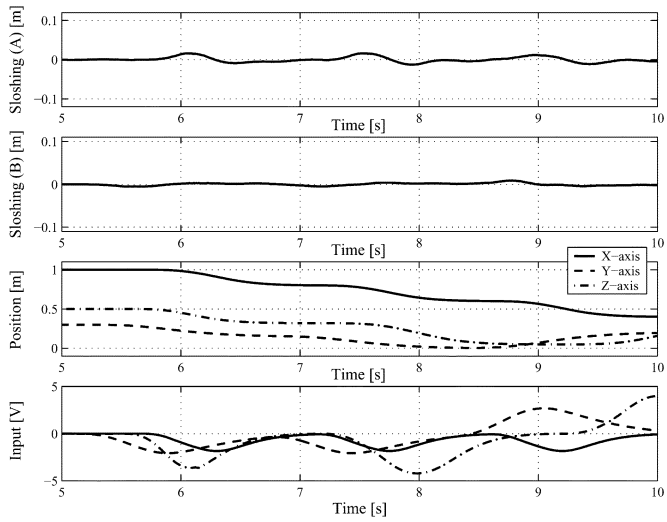

Fig. 18. Experimental result of container transfer by the Hybrid shape approach for random reference endpoints.

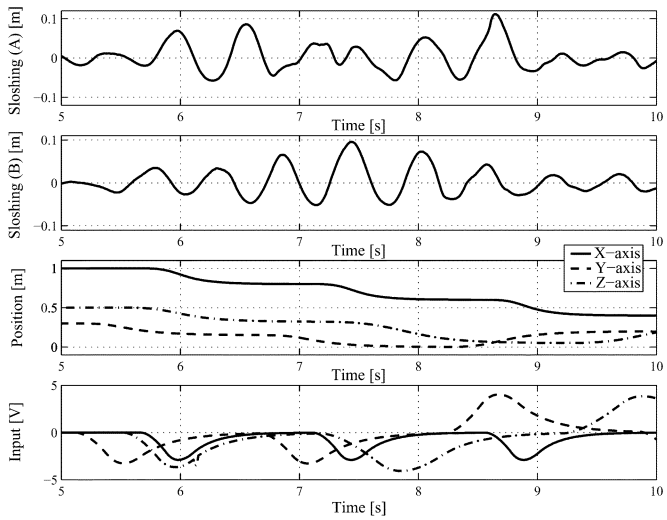

Fig. 19. Experimental result of container transfer by the P control for random reference endpoints.

The maximum amplitude of the sloshing reached about 3.5 times on the X axis and about 10 times on the Y axis, compared with the results shown in Fig. 8. If the container had been full of liquid, overflow would have occurred.

VI. Conclusion

This paper presents a control design method, called the Hybrid shape approach, for trajectory control with vibration damping on transfer systems with vibration mechanisms.

The control design method was applied to a liquid container on a 3-D transfer path. The results demonstrated that the position control system satisfies the various control specifications in both the time and frequency domains, using only feedback on the container's position. The effectiveness of the control design method was shown by control experiments. Also, the problem of suppressing sloshing in a liquid container transfer system that can freely transfer a container in 3-D space has been solved. This result can contribute greatly to the realization of space-saving factories, to the optimization of production processes and to the improvement of productivity in real industries.

References

[1] K. Yano and K. Terashima, "Robust liquid container transfer control for complete sloshing suppression," *IEEE, Trans. Contr. Syst. Technol.*, vol. 9, no. 3, pp. 483–493, May 2001.

[2] J. T. Feddema *et al.*, "Control for slosh-free motion of an open container," *IEEE Contr. Syst. Mag.*, vol. 17, no. 1, pp. 29–36, Feb. 1997.

[3] M. Hamaguchi, K. Terashima, and H. Nomura, "Optimal control of liquid container transfer for several performance specifications," *J. Adv. Automat. Technol.*, vol. 6, pp. 353–360, 1994.

[4] K. Terashima and K. Yano, "Sloshing analysis and suppression control of tilting-type automatic pouring machine," *IFAC J. Contr. Eng. Practice*, vol. 9, no. 6, pp. 607–620, 2001.

[5] W. Lindsay, "Automatic pouring and metal distribution system," *Foundry Trade J.*, pp. 151–165, 1983.

[6] Y. Lerner and N. Laukhin, "Development trends in pouring technology," *Foundry Trade J.*, vol. 11, pp. 16–21, 2000.

[7] M. Grundelius and B. Bernhardsson, "Motion control of open containers with slosh constraints," in *Proc. 14th IFAC World Congress*, Beijing, China, 1999, pp. 487–492.

[8] ——, Constrained iterative learning control of liquid slosh in an industrial packaging machine. presented at *Proc. IEEE Conf. Decision Contr.*

[9] M. Hamaguchi, M. Yamamoto, and K. Terashima, "Modeling and control of sloshing with swirling in a cylindrical container during a curved path transfer," in *Proc. Asian Contr. Conf.*, Tokyo, Japan, 1997, pp. 233–236.

[10] K. Yano, S. Higashikawa, and K. Terashima, "Motion control of liquid container considering an inclined transfer path," *IFAC J. Contr. Eng. Practice*, vol. 10, no. 4, pp. 465–472, 2002.

[11] N. Singer and W. Seering, "Preshaping command inputs to reduce system vibration," *J. Mech. Design*, vol. 112, pp. 76–82, 1990.

[12] W. Singhose, W. Seering, and N. Singer, "Residual vibration reduction using vector diagrams to generate shaped inputs," *J. Mech. Design*, vol. 116, pp. 654–659, 1994.

[13] L. Collatz and W. Wetterling, "Optimization problems," in *Applied Mathematical Sciences*. New York: Springer-Verlag, 1975, vol. 17.

Ken'ichi Yano (S'98–A'99–M'01) was born in Osaka, Japan, in 1969. He received the B.E. degree, the M.E. degree in production systems engineering, and the D.E. degree in electronic and information engineering from Toyohashi University of Technology, Aichi, Japan, in 1994, 1996, and 1999, respectively.

He has been with Gifu University, Gifu, Japan, since 2004 as an Associate Professor. He was a Visiting Research Fellow with the Technical University of Berlin, Berlin, Germany, from August 2002 until August 2003. His research interests include control theory and its applications to transfer systems, industrial robots, and medical systems.

Kazuhiko Terashima (S'79–M'81) was born in Osaka, Japan, in 1952. He received the B.S. and M.S. degrees from the Kyoto Institute of Technology, Kyoto, Japan, in 1976 and 1978, respectively, and the Ph.D. degree in mechanical engineering from Kyoto University, Kyoto, Japan, in 1982.

Since 1982, he has been with Toyohashi University of Technology, Aichi, Japan, and he has been a Professor since 1994. He was a Visiting Research Fellow with the Technical University of Munich, Munich, Germany, from September 1991 until September 1992. His research interests lie in the analysis and design of control systems and the application to motion control, robotics, and intelligent systems.